Monochromatic aberrations in resonant optical elements applied to a focusing multilevel reflectarray

James Ginn[1], Javier Alda[2], José Antonio Gómez-Pedrero[2], Glenn Boreman[1,*]

[1]*CREOL. University of Central Florida. 4000 Central Florida Blvd. Orlando. FL 32816-2700. USA*
[2]*Applied Optics Complutense Group. University Complutense of Madrid. Arcos de Jalón, 118. 28037 Madrid. Spain*
**boreman@creol.ucf.edu*

Abstract: The monochromatic aberrations produced by the phase distribution reflected by resonant sub-wavelength metallic structures are studied both analytically and numerically. Even for normal incidence, the angular dependence of the re-radiated wavefront disturbs the overall performance of the reflectarray. This effect is modelled as combination of a linear and a cubic dependence. A complete numerical simulation of a multilevel focusing reflectarray is performed using computational-electromagnetic and physical-optics-propagation methods. A modified Strehl ratio is defined to show the dependence of the focused spot behavior on aperture. The irradiance distribution is dependent on the polarization state. A small-aperture focusing reflectarray has been designed, fabricated, and tested. The irradiance distribution at the focusing plane is compared with the simulated one, showing a good agreement when residual wavefront aberrations are included.

OCIS codes: 160.3918 (materials; metamaterials); 050.5080 (diffraction and gratings; phase shift); 110.3080 (imaging systems; infrared imaging)

References and Links

1. B. Munk, "Finite Antenna Arrays and FSS," Wiley (2006)
2. J. S. Tharp, J. M. Lopez-Alonso, J. C. Ginn, C. F. Middleton, B. A. Lail, B. A. Munk, and G. D. Boreman, "Demonstration of a single-layer meanderline phase retarder at infrared," Opt. Lett. **31**(18), 2687–2689 (2006).
3. D. Berry, R. Malech, and W. Kennedy, "The reflectarray antenna," IEEE Trans. Antenn. Propag. **11**(6), 645–651 (1963).
4. J. Montgomery, "Scattering by an infinite periodic array of microstrip elements," IEEE Trans. Antenn. Propag. **26**(6), 850–854 (1978).
5. D. Pozar, and T. Metzler, "Analysis of a reflectarray antenna using microstrip patches of variable size," Electron. Lett. **29**(8), 657–658 (1993).
6. F. González, J. Alda, J. Simón, J. Ginn, and G. Boreman, "The effect of metal dispersion on the resonance of antennas at infrared frequencies," Infrared Phys. Technol. **52**(1), 48–51 (2009).
7. J. Ginn, B. Lail, and G. Boreman, "Phase characterization of reflectarray elements at infrared," IEEE Trans. Antenn. Propag. **55**(11), 2989–2993 (2007).
8. J. Ginn, B. Lail, J. Alda, and G. Boreman, "Planar infrared binary phase reflectarray," Opt. Lett. **33**(8), 779–781 (2008).
9. F. Shen, and A. Wang, "Fast-Fourier-transform based numerical integration method for the Rayleigh-Sommerfeld diffraction formula," Appl. Opt. **45**(6), 1102–1110 (2006).
10. M. Young, "Zone plates and their aberrations," J. Opt. Soc. Am. **62**(8), 972–976 (1972).
11. H. Hristov, "Fresnel zones in wireless links, zone plates lenses and antennas," Artech (2000)
12. M. Y. Kiang, "Neural networks," in Encyclopedia of Information Systems, Academic Press (2002), 303–315.
13. J. H. McLeod, "Axicons and their uses," J. Opt. Soc. Am. **50**(2), 166–166 (1960).
14. J. S. Tharp, J. Alda, and G. D. Boreman, "Off-axis behavior of an infrared meander-line waveplate," Opt. Lett. **32**(19), 2852–2854 (2007).
15. V. Mahajan, "Aberration theory made simple," SPIE Press (1991).
16. Y. Li, and E. Wolf, "Focal shift in diffracted converging spherical waves," Opt. Commun. **39**(4), 211–215 (1981).

#124181 - $15.00 USD Received 11 Feb 2010; revised 3 Apr 2010; accepted 5 Apr 2010; published 10 May 2010

1. Introduction

Refractive or reflective optical elements are based on physical interfaces separating dielectric or metallic materials. They are the components of most conventional optical systems. Evaluations of optical path differences and wavefront distortions are made within the framework of classical optical aberrations. Diffractive optical elements are also widely used, alone or in combination with refractive optics, creating new degrees of freedom in optical design problems. As appropriate, scalar or vector propagation and interference laws model these elements. In this contribution we introduce a new kind of optical element based on the resonance of subwavelength metallic structures [1,2]. The metallic elements have geometric details well under the wavelength value. The resonance that is used in these structures is given by the cooperative effect of the regularly arranged elements. This resonant behavior may change the spectral distribution, the polarization state or the phase of the output wavefront. These can be configured as reflective or transmissive elements, and can be fabricated on a flat or conformal surface. The concept has been adapted from the radiofrequency portion of the spectrum where they are known as reflectarrays when denoting reflecting elements [3–5]. However, when moving to higher frequencies, the optical properties of materials at sub-wavelength dimensions makes them behave as imperfect conductors [6]. This behavior changes the performance of these elements at infrared and optical frequencies.

The fundamentals of resonant optical elements for phase-shaping applications are based on the interaction of the electromagnetic waves with metallic structures arranged as a quasi-periodic pattern. Due to this resonant interaction, for a given geometry and material arrangement, the phase shaping depends on the wavelength, the angle of incidence, and the polarization state of the incoming wavefront. These dependences are intrinsically different from those obtained for refractive and diffractive optical systems. The capability to induce a phase shift by sub-wavelength resonant elements in the infrared was demonstrated for the material and the geometry used in this contribution [7]. Starting from that article an infrared reflectarray was fabricated and successfully characterized using a Soret configuration and resonant elements showing a π phase shift with respect to the phase produced by the ground plane [8]. With these previous results, an improvement in the design for better efficiency was proposed and realized in the form of a multilevel reflectarray acting as a focusing mirror. Figure 1 shows the structure of the sub-wavelength elements. The element is defined on a unit cell having a constant size along the reflectarray. In our case the unit cell is a $5 \times 5\ \mu m^2$ square. A stand-off layer is grown on a metallic ground plane. On top of the stand-off layer, a metallic patch is deposited. The form and size of this metallic patch determines the phase shift given by the region of the reflectarray containing this individual element. The photographs of Fig. 1 show a square patch and also a slotted square patch of the type used to build a multilevel reflectarray.

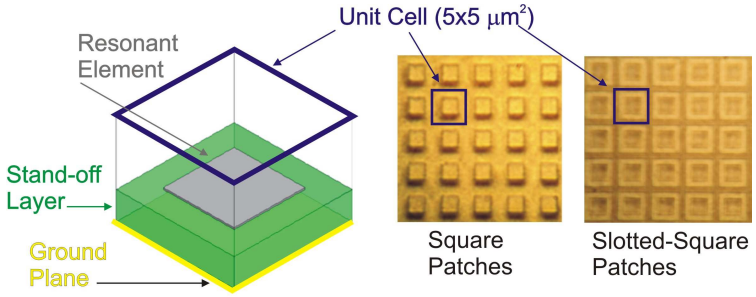

Fig. 1. The unit cell for an individual resonant element is sketched on the left of the figure. The visible microscope photographs show two geometries for the metallic patches of the resonant elements: squares, and slotted squares.

In this contribution we evaluate the phase dependences with respect to angle of incidence and polarization state for a fixed wavelength. Our analysis is performed for resonant optical elements fabricated with square and square-slotted unit-cell designs arranged as a multilevel

#124181 - $15.00 USD Received 11 Feb 2010; revised 3 Apr 2010; accepted 5 Apr 2010; published 10 May 2010

Fresnel zone plate. Section 2 presents an approximate analytical model of some monochromatic aberrations of a reflectarray, under normal incidence conditions. In section 3, this analysis is extended by a numerical simulation of the phase shift as a function of the reflected angle and polarization state. The reflectarray is modeled as a phase screen and the reflected wavefront is propagated by a Rayleigh-Sommerfeld algorithm [9]. The analysis is performed under both small- and large-aperture conditions. Experimental results obtained from a small-aperture reflectarray are compared with the numerical results. Section 4 summarizes the main conclusions of the paper.

2. Analytical solution for an on-axis reflectarray system

The analysis of the aberration of a reflectarray begins with evaluation of the optical-path differences as a function of the location of the subwavelength element within the array. First, we present an analysis applicable to an off-axis incidence. The on-axis results are then obtained from it. Using a purely geometric approach, this location (in a Fresnel-zone arrangement), depends on the radial coordinate $r = \sqrt{x^2 + y^2}$, with (x,y) as the coordinates within the reflectarray plane, the focal length, f', and the angle of incidence, α. The phase difference can be related with the previous geometric quantities as follows:

$$\begin{aligned} \Phi &= \frac{2\pi}{\lambda}\left\{ r\sin\alpha + f'\left[\sqrt{1+\left(\tan\alpha - \frac{r}{f'} \right)^2} - \sqrt{1+\tan^2\alpha} \right] \right\} \\ &\approx \frac{2\pi}{\lambda}\left[\frac{r^2}{2f'} - \frac{r^4}{8f'^3} + \frac{r^3\alpha}{2f'^2} - \frac{3r^3\alpha^2}{4f'} \right], \end{aligned} \tag{1}$$

where the approximate result given in the second line has been obtained by series expansion of the square root and the trigonometric functions [10,11]. The four terms in the square brackets of this equation can be identified as follows: the first one is the paraxial approximation to a spherical wavefront, the second term is spherical aberration, the third term is astigmatism and field curvature, and the fourth term is coma. Only the two first terms are different from zero for normal incidence, $\alpha = 0$.

Equation (1) only computes optical-path differences. For a reflectarray, besides these geometrical terms, an additional term describing the changes in phase introduced by the resonant patches has to be included. If all the geometrical aberrations were to be corrected, this residual wavefront error induced by the resonant elements would remain. When considering a monochromatic wave, this additional term depends on the angular behavior of the reflected field. This additional phase shift can be modelled as two terms,

$$\Phi_{additional} = \Phi(\alpha) + \Phi(\theta). \tag{2}$$

The first term depends on the angle of incidence, α, and the second term depends on the angle θ defined by the line joining a particular subwavelength element and the focal point, and the normal line to the reflectarray surface (see Fig. 2). In the following we will interested in the on-axis incidence, i.e., $\alpha = 0°$. Actually, θ can be easily related with the location at the reflectarray plane as,

$$\theta = \tan^{-1}\left(\frac{r}{f'} \right) \approx \frac{r}{f'} - \frac{1}{3}\left(\frac{r}{f'} \right)^3, \tag{3}$$

up to a third-order expansion. This angle, θ, will be referred to as the aperture angle in this paper. Even for normal incidence conditions, $\alpha = 0$, the second term of Eq. (2) does not vanish. It represents the phase shift observed in the re-radiated wavefront at a given direction defined by θ. This phase shift, $\Phi(\theta)$, can be calculated using computational-electromagnetic

#124181 - $15.00 USD Received 11 Feb 2010; revised 3 Apr 2010; accepted 5 Apr 2010; published 10 May 2010

methods and it depends not only on the angle θ, but also on the orientation of the incident electric field (the incoming polarization state of the electromagnetic wave).

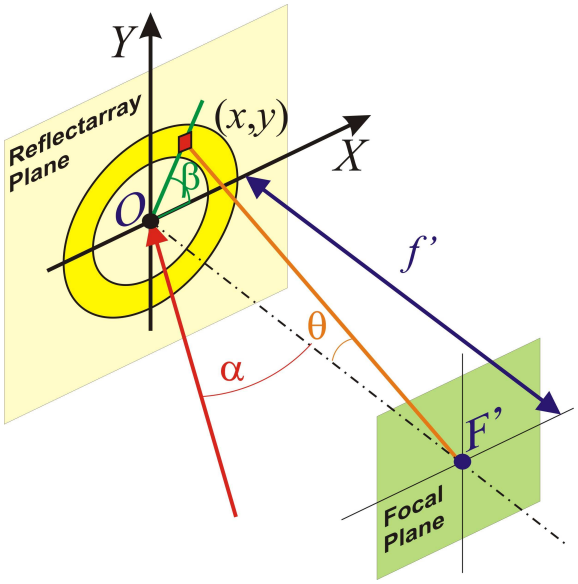

Fig. 2. Typical layout of a reflectarray focusing onto a plane. The resonant element is represented as the red square on a circular ring at the reflectarray plane having coordinates (x,y) with respect to the origin of the reflectarray O. The focal plane is situated at a distance f' from the reflectarray plane. Angles θ and β are the elevation and azimuth angles respectively. They describe the location of a given point of the reflectarray with respect to the focal point of the system, F'. The angle α is the angle of incidence of the incoming beam with respect to the optical axis.

The numerically computed results for $\Phi(\theta)$ are shown and discussed in the next section assuming normal incidence, $\alpha = 0$ (see Fig. 2). Here we present an approximate form for the angular dependence of the phase shift analytically modelled using a sigmoid function [12]. Some other analytical functions can be proposed for this fitting. A sigmoid function is chosen since it has also been used to model the dependence of the phase shift with the size of the square patch in the unit cell [7]. Independently of the type of function used, the analytical fitting, and its power expansion, provides a simple connection between the geometric-aberration theory and this new contribution to the wavefront error. As a possible form for this sigmoid we propose the following one

$$\Phi(\theta) = \Phi_0 + \frac{A}{1+\exp\left(-\left|\frac{\theta}{B}\right|\right)}, \tag{4}$$

where Φ_0, A, and B are fitting constants. Although a more accurate description of the angular effects will need a computational approach, the modelling using an analytic function makes possible some useful interpretation of the angular phase dependence. Using Eq. (4) to represent this dependence, and after expanding in powers of θ, we obtain:

$$\Phi(\theta) = \Phi_0 + A\left[\frac{1}{4}\frac{\theta}{B} - \frac{1}{48}\left(\frac{\theta}{B}\right)^3\right], \tag{5}$$

this, by using Eq. (3), can be written as a function of r,

#124181 - $15.00 USD Received 11 Feb 2010; revised 3 Apr 2010; accepted 5 Apr 2010; published 10 May 2010

$$\Phi(r) = \Phi_0 + A\left[\frac{1}{4}\frac{r}{Bf} - \frac{4B^2+1}{48B^3}\left(\frac{r}{f'}\right)^3\right]. \quad (6)$$

The first term in the square bracket is linear with r, and can be explained as an axicon-type phase dependence [13]. The second term is a third-order aberration similar in symmetry to spherical aberration, but having a cubic dependence on aperture instead of the usual 4th-power dependence. In situations where the angular dependence may depend on the polarization of the incident field (as happens with meander-line structures [14]), the fitting coefficients A and B in Eqs. (4)-(6), may change when considering the polarization state of the incoming light.

The previous analysis has some limitations. The most important is that the postulated angular behavior is applicable piece-wise over the reflectarray plane, the pieces defined by the regions where the same subwavelength resonant element is written. When moving to a different region populated with different resonant elements, the constants Φ_0, A, and B have to be changed. Besides that, a complete analysis of this aberration behavior will imply more detailed dependences with respect to the polarization state of the incident light and the local decomposition in TE and TM modes on the reflectarrray plane. However, with this approximate analytical model we have shown that the resonant elements introduce by themselves some intrinsic aberrations. The total aberration function contributed by these elements should include these new terms. The new degrees of freedom thus generated may ultimately prove to be of some benefit for balancing other aberrations present in the system.

3. Computational modeling of a multi-level reflectarray focusing mirror

The modeling of the angular and polarization response has been made using two different computational tools: a finite-element package (HFSS by Ansoft) and a method-of-moments algorithm (Designer by Ansoft). For our present situation, we are interested in the angular dependence of the resonant elements. With this in mind we have calculated the irradiance distribution at the focal point of the resonant optical element, by modeling the resonant optical element as a phase screen. The phase screen has a dependence as follows:

$$\Phi = \Phi(x, y, \lambda, \theta, s), \quad (7)$$

where, x and y are the spatial coordinates on the plane of the phase screen, λ is the wavelength, θ denotes the angle of the optical path with respect to the normal to the surface, and s represents the polarization state. As far as we are presently interested in the monochromatic dependences we will assume λ as a constant and consequently drop it from the dependence.

After demonstrating the focusing capabilities of a focusing reflectarray with a binary phase FZP [8], we have upgraded the design into a multilevel Fresnel subzone arrangement, where the phase shift is distributed over the 2π range. The zone boundaries are determined from diffractive considerations, and the actual dimensions of the individual elements are obtained from the computational-electromagnetic results. The goal is to optimize behavior for normal incidence conditions. Therefore, the aberration analysis, including the effect of the resonant elements, is of primary importance. This is why the variations of the phase shift with angle and polarization state have been calculated. All these dependences are plotted in Fig. 3.a and Fig. 3.b that show the modulus and the phase for the eight discrete phase-step elements used in this design. These modulus and phase values define a complex reflectivity, ρ, for each polarization component. The complex reflectivity has been obtained from the computational electromagnetic results, and could be calculated for any other geometry or spectral range. Therefore, although illustrated here for a specific reflectarray unit cell, this treatment and analysis method can be considered applicable in general.

#124181 - $15.00 USD Received 11 Feb 2010; revised 3 Apr 2010; accepted 5 Apr 2010; published 10 May 2010

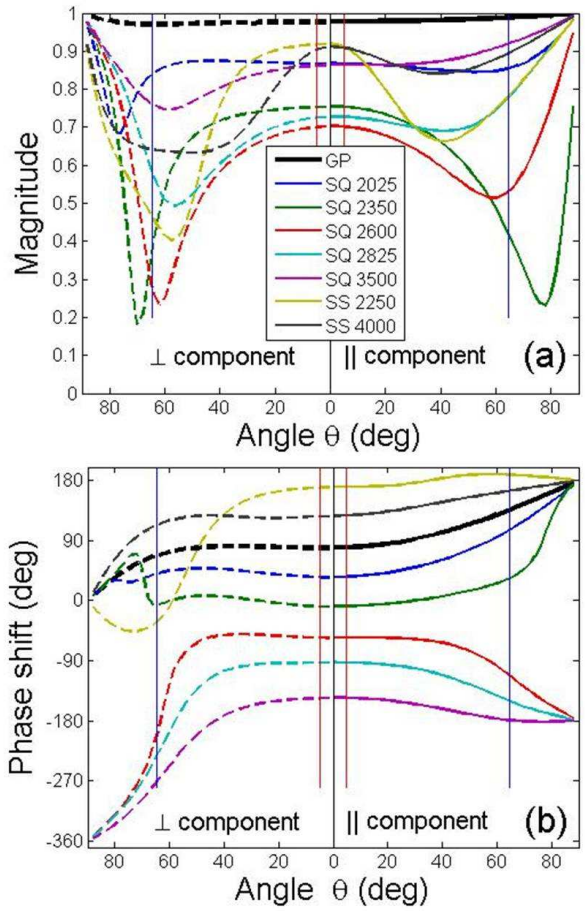

Fig. 3. Magnitude (top) and phase shift (bottom) produced by the eight elements of the subzone as a function of the angle and the polarization state (TE, perpendicular, and TM, parallel, components). The color coding is the same for both graphs. The labels are GP for the ground plane, and SQ for the square patches, being the number the size of the patch in nm, and SS for square slotted patches, being the number the size of the slot in a 4500 nm square patch. The vertical lines correspond with the maximum value of θ for the small aperture (red) and large aperture (blue) reflectarrays referred in the text.

From these figures we see that the phase remains quite constant for an angular range of about ± 20 degrees. This corresponds quite well with the paraxial range that is commonly used in conventional optical design. This general behavior was also obtained when checking the angular application range of meander-like resonant structures for polarization control [14]. Then, the phase shift begins to depart from the one obtained at normal incidence. Even larger variations are observed in the modulus of the reflectance. Besides, although the patches are designed as square so as to have not a preferential state of polarization, when we go towards larger angles, we see that the TE (perpendicular component) and TM (parallel component) states of polarization behave differently. This situation is treated using a Jones-matrix formalism. The two components of the Jones vector are treated as spatial maps of a complex electric field. These components are transformed as follows:

$$\begin{pmatrix} E_{x,out}(x,y) \\ E_{y,out}(x,y) \end{pmatrix} = R(-\beta(x,y)) \begin{pmatrix} \rho_{\parallel,\parallel}(x,y) & \rho_{\parallel,\perp}(x,y) \\ \rho_{\perp,\parallel}(x,y) & \rho_{\perp,\perp}(x,y) \end{pmatrix} R(\beta(x,y)) \begin{pmatrix} E_{x,in}(x,y) \\ E_{y,in}(x,y) \end{pmatrix}. \quad (8)$$

#124181 - $15.00 USD Received 11 Feb 2010; revised 3 Apr 2010; accepted 5 Apr 2010; published 10 May 2010

The incoming map of the electric field, characterized by the two components of the electric field, is transformed by the complex reflection coefficients, $\rho(x,y)$. They behave differently for each subzone of the reflectarray because the patches are different. When considering the calculation for the focal point and its neighborhood the angular dependence on θ can be transformed into a x,y dependence. These reflection coefficients are different for each polarization orientation with respect to the incidence plane. Besides, this polarization state changes along the reflectarray plane. For example, a given $E_{x,in}$ component will move from a parallel component when impinging at those locations having $y = 0$ ($\beta = 0°$), to a perpendicular component for the locations on the reflectarray at $x = 0$ ($\beta = 90°$). The dependence with β is represented by the two rotation matrices $R(\beta)$, and $R(-\beta)$, where β is also a function of the location at the reflectarray plane (see Fig. 1). In our numerical simulations we will neglect the contribution from the cross-polarization coefficients ($\rho_{\parallel,\perp} = \rho_{\perp,\parallel} \approx 0$). The angular dependence of $\rho_{\parallel,\parallel}$ (TM mode) and $\rho_{\perp,\perp}$ (TE mode) are obtained from the calculated values represented in Fig. 2. The two components of the field obtained after the phase screen are propagated to the focal plane by using a Rayleigh-Sommerfeld algorithm [9]. The results have been obtained for two reflectarrays having different aperture. One of them is a small-aperture focusing mirror constructed with 100 Fresnel semiperiodic zones and having a focal length $f' = 0.152$ m and an $F/6$ aperture. The maximum value of θ for this element is $\theta_{max} = 4.76°$. The other element is more extreme design having 200 Fresnel semiperiodic zones and a focal length of $f' = 800$ μm. Here, the $F\#$ is much lower and the system is having an F/0.24 aperture. Then, the maximum value of the angle involved in the calculation is $\theta_{max} = 64.66°$, a value that is clearly far away from the paraxial regime.

The contribution from the angular and polarization dependences is given as a modified Strehl ratio that we have calculated as a function of the aperture angle, θ. The Strehl ratio is usually defined as the quotient between the observed maximum irradiance at the focal point, and the theoretical maximum irradiance at the same point for the diffraction-limited case [15]. This ideal case is taken as the reference and a larger Strehl ratio means a better performance. In this contribution, we have modified the reference value of the Strehl ratio to properly account for the different terms degrading the performance of the reflectarray. For the small-aperture reflectarray we have defined the reference for this Strehl ratio as follows. It is the irradiance obtained at the nominal focal point for an ideal reflectarray having a uniform reflectance with modulus equal to one, and 8 phase levels shifted consecutively by π/4. Figure 4.a shows this Strehl ratio when considering the change in amplitude and phase due to the angular dependence applied to the small-aperture F/6 system. The value of this parameter is almost constant and close to 0.7 for the elements considered. This is mainly due to the value of the modulus of the reflectance coefficient shown in Fig. 3.a. By using this modified Strehl ratio we account for the discrepancies in amplitude and phase with respect to the ideal case. The irregularities observed for the first zones are due to the presence of focal shifts with respect to the nominal focus where we evaluate the irradiance [16]. The maximum angle involved in this design corresponds to the nearly flat region around $\theta = 0°$ for amplitude and phase (see Fig. 3). Hence, Fig. 4.a mostly describes the variability in magnitude of the subzone contributions, and the discrepancies of the consecutive phase shift from the ideal π/4 value.

#124181 - $15.00 USD Received 11 Feb 2010; revised 3 Apr 2010; accepted 5 Apr 2010; published 10 May 2010

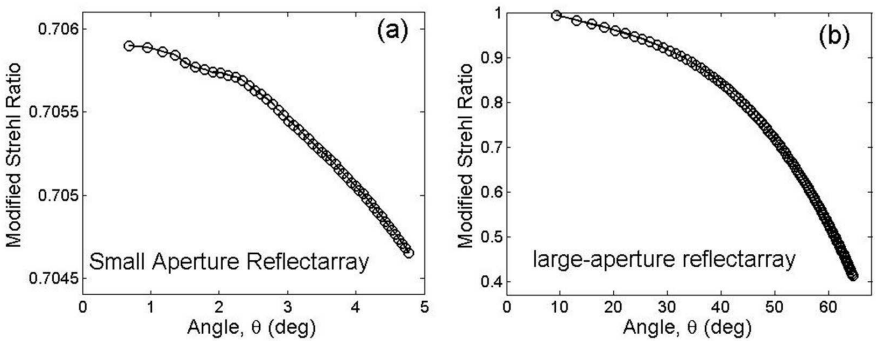

Fig. 4. Modified Strehl ratio as a function of the aperture angle θ. On the left (a) we have represented the small-aperture reflectarray. The maximum reflection angle is 4.77°. The figure at the right (b) is for the larg- aperture reflectarray that reaches an angle of 64.66°. The modified Strehl ratio has been calculated at discrete points, represented by circles. The solid line joining the circles has been validated numerically, and represents the smoothness and continuity of the dependence.

As we mentioned before, in order to recognize the effect of the angular and polarization dependence of the resonant elements, we have simulated a more extreme situation realized with a very low F# element having a diameter of 3.38 mm and a short focal length of 0.8 mm. The maximum angle of incidence is now 64.66°. This design shows a strong angular dependence that is plotted in Fig. 4.b. Here the reference to represent the modified Strehl ratio is given by the irradiance at the focal point obtained for a reflectarray showing a constant value of the complex reflectance, independently of the aperture angle θ. The values of the complex reflectance of this reference (magnitude and phase) are those obtained at $\theta = 0°$, showing no polarization dependence. Thus, our normalization accounts for the angular dependence.

The dependence with the polarization state of the incoming light is not noticeable for the case of a small-aperture system. Also, when calculating the modified Strehl ratio for different azimuth angles of the incident linear polarization state no significant variations are observed in this parameter for both reflectarrays considered here (small and large aperture)

However, the shape of the focal spot shows a clear dependence on the polarization state. The dependence in shape also appears for the small-aperture case, but it is not noticeable and can be neglected. The results for the large-aperture reflectarray are shown in Fig. 5. We have represented the central portion of the focal spot for three representative cases. The irradiance distribution is obtained from the calculation of the reflected electric field components using Eq. (8). Then, the two orthogonal electric field distributions are propagated to the focal plane using a Rayleigh-Sommerfeld algorithm. Then, after obtaining the maps of the components of the electric field at the focal plane, the irradiance is easily obtained as the squared modulus of the resulting electric field. On the left we show a circularly symmetric spot obtained when no polarization dependence is present. The central spot is for a linearly polarized wavefront aligned along the horizontal axis ($E_{y,in}(x,y) = 0$). The spot in the right shows the results for a linearly polarized wavefront having a 45° azimuth orientation.

#124181 - $15.00 USD Received 11 Feb 2010; revised 3 Apr 2010; accepted 5 Apr 2010; published 10 May 2010

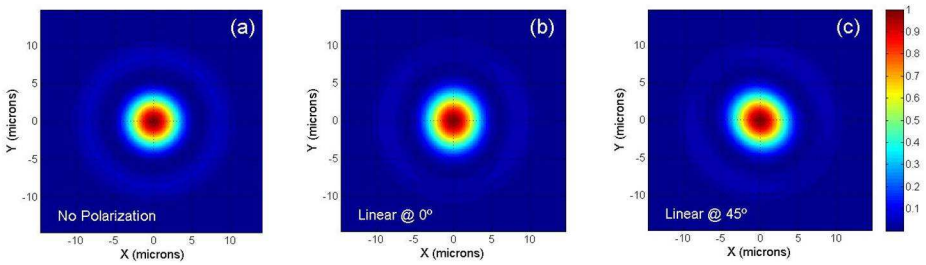

Fig. 5. Irradiance distribution at the focal plane of a large-aperture reflectarray for three different cases. a) No polarization dependence, b) linear polarization at an azimuth of 0°, and c) linear polarization with azimuth of 45°. The colormap is the same for the three figures and it is normalized to the maximum of the irradiance.

The element actually fabricated and tested is one having a small aperture of F/6. We have simulated the distribution at the focal point of this element. The results are shown in Fig. 6. The experimental distribution has been obtained using a pyroelectric camera having a pixel pitch of 100 μm. The simulated spot has been obtained adding 2 waves of spherical aberration and slightly displacing the center of the calculated beam with respect to the center of the central pixel of the camera. The simulated irradiance is sampled and integrated within the pixel area to obtain a distribution that could be compared with the experimental one. Spherical aberration is included because of the optical train used to illuminate the reflectarray. This is comprised of two positive meniscus lenses in the form of an inverted telescope. The laser beam is actually filling the whole aperture of the second lens. Also the wafer used for fabricating the reflectarray was not optically flat. It shows a fringe distribution revealing an astigmatic asphericity of about 2 wavelengths from the center to the edge of a 5 cm wafer. Other impacts on the shape and extent of the focal spot may arise from the Gaussian beam that is delivered by the CO_2 laser. This beam is specified as having M^2 = 1.1. Therefore, the illuminating beam also contributes to the wavefront error.

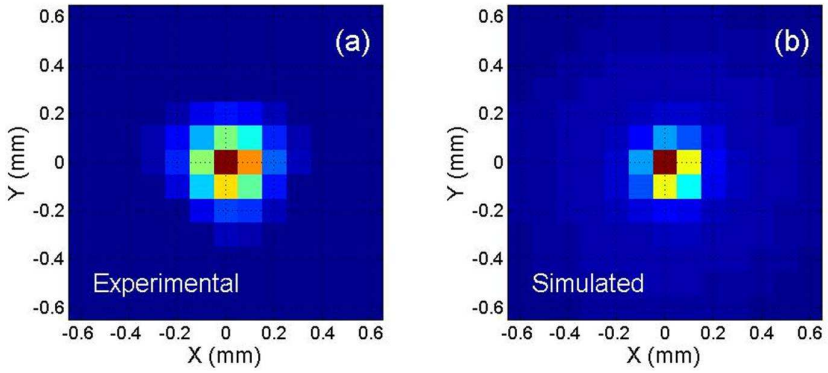

Fig. 6. Experimental (a) and calculated (b) irradiance distribution onto a pyroelectric camera.

4. Conclusions

Reflectarrays are optical elements that modify the incoming phasefront using resonant metallic structures having subwavelength dimensions. It is possible to customize the geometry of these structures to produce a desired phasefront. The reflected amplitude, both in magnitude and phase, has been evaluated as a function of the wavelength and the polarization state.

A simple analytic model of the aberrations produced by the reflectarrray elements has been presented and discussed. Besides the geometrical aberrations, the angular dependence of the phase shift produced by the resonant sub-wavelength is present even for normal incidence

#124181 - $15.00 USD Received 11 Feb 2010; revised 3 Apr 2010; accepted 5 Apr 2010; published 10 May 2010

conditions. The angular dependence of the phase shift is modeled using a series expansion of a sigmoid function. The terms of the expansion can be interpreted as a linear phase (axicon-type) plus a cubic dependence on aperture height. Although the limitations of this analytic model motivate a complete electromagnetic simulation of the actual behavior of the resonant elements, this simple model helps to show that there is a new term whose contribution adds to the classical geometric aberrations. A more complete picture is provided by the computational-electromagnetic results, which describe the angular dependence for each selected geometric parameter. Both amplitude and phase are calculated. Also, the dependence of the amplitude and phase is split in the two possible components of the incoming electric field with respect to the incidence plane: transverse magnetic (TM or parallel component) transverse electric (TE or perpendicular component). The complex reflection coefficient derived from these calculations describes the behavior of the reflectarray element and can be obtained for any other geometry or situation. The complex reflectivity map of the reflectarray is obtained in a piece-wise fashion over the Fresnel zone arrangement.

This analysis has been applied to a reflectarray having eight phase zones regularly distributed in phase along the 2π interval. The phase shifts are calculated from the computational electromagnetic analysis. The aberration of the reflectarray is evaluated as a function of the aperture size (parameterized in terms of the aperture angle subtended by the focal point from the outer edge of the reflectarray). A modified Strehl ratio is defined to account for the angular effect that is more relevant as the aperture increases. This is because the angles involved to focus the light are larger for larger apertures. However, when changing the polarization state of the incoming light no relevant changes in the value of the Modified Strehl ratio are observed. The polarization state changes the shape of the irradiance distribution around the focus, as we have shown for a large-aperture reflectarray. The focused spot becomes slightly asymmetric and rotates with the azimuth of the linearly polarized light.

Using our simulation procedure, a small-aperture eight-subzone focusing mirror has been designed, fabricated, and tested. The experimental and simulated results fit quite well, and the origin of the discrepancies has been identified: spherical aberration from the illuminating optical train, surface deformation of the reflectarray substrate, and the departure from strict Gaussianity of the incident laser beam.

In summary, we have described the focusing behavior of an optical element fabricated with resonant structures. The nature of these resonances makes this element dependent upon the polarization state and the aperture of the element. The actual modeling of this dependence is strongly dependent on the geometry and material characteristics of the sub-wavelength resonant elements.

Acknowledgments

This work has been partially supported by the Spanish Ministry of Science and Innovation through projects TEC2006-01882 and ENE2009-14340-C02-01.

#124181 - $15.00 USD Received 11 Feb 2010; revised 3 Apr 2010; accepted 5 Apr 2010; published 10 May 2010